

We are IntechOpen, the world's leading publisher of Open Access books Built by scientists, for scientists

6,900

Open access books available

186,000

International authors and editors

200M

Downloads

Our authors are among the

154

Countries delivered to

TOP 1%

most cited scientists

12.2%

Contributors from top 500 universities



WEB OF SCIENCE™

Selection of our books indexed in the Book Citation Index
in Web of Science™ Core Collection (BKCI)

Interested in publishing with us?
Contact book.department@intechopen.com

Numbers displayed above are based on latest data collected.
For more information visit www.intechopen.com



Hyperbranched Polyimides Prepared from 4,4',4''-Triaminotriphenylmethane and Mixed Matrix Materials Based on Them

Evgenia Minko, Petr Sysel, Martin Spergl and Petra Slapakova

Additional information is available at the end of the chapter

<http://dx.doi.org/10.5772/2834>

1. Introduction

Polymers are macromolecules built up by the linking together, under formation of chemical bonds, of large numbers of much smaller molecules (monomers). Due to their structure they can be classified as linear, branched, or crosslinked polymers [1]. The dendritic topology (dendrimers, hyperbranched polymers) has recently been recognized as a new class of macromolecular architecture. Dendritic polymers are expected to play a key role as enabling building blocks for nanotechnology during the 21st century [2].

Hyperbranched polymers are highly branched macromolecules. The highly branched structure and a large number of terminal functional groups, resulting, e.g., in better solubility and lower viscosity, are their important structural features which distinguish them from linear polymers. They do not have the perfectly branched architectures but they are thought to have similar physical properties to dendrimers and for some cases they can be used to replace them. (Dendrimers consist of highly branched, monodisperse spherical macromolecules containing a control core surrounded by repeating units, all enclosed by a terminal group shell. They are prepared using multi-step syntheses [2]). Hyperbranched polymers often can be simply prepared by a direct one-step polymerization of multifunctional monomers using a single-monomer (starting compound is generally AB_x monomer, most frequently AB_2 (Figure 1)) or double-monomer (A_2+B_3) methodology [3]. (A and B represent two kinds of functional groups which can react with each other but cannot undergo self-reaction.) Many kinds of hyperbranched polymers, e.g., polyesters, polyethers, poly(ether ketone)s, poly(ether sulfone)s, polyamides, have been investigated as novel dendritic macromolecules so far [3]. An increasing attention has been also devoted to hyperbranched polyimides [4] due to a potentially possible connection of the known advantages of linear or crosslinked polyimides [5] with those of hyperbranched polymers [2,3].

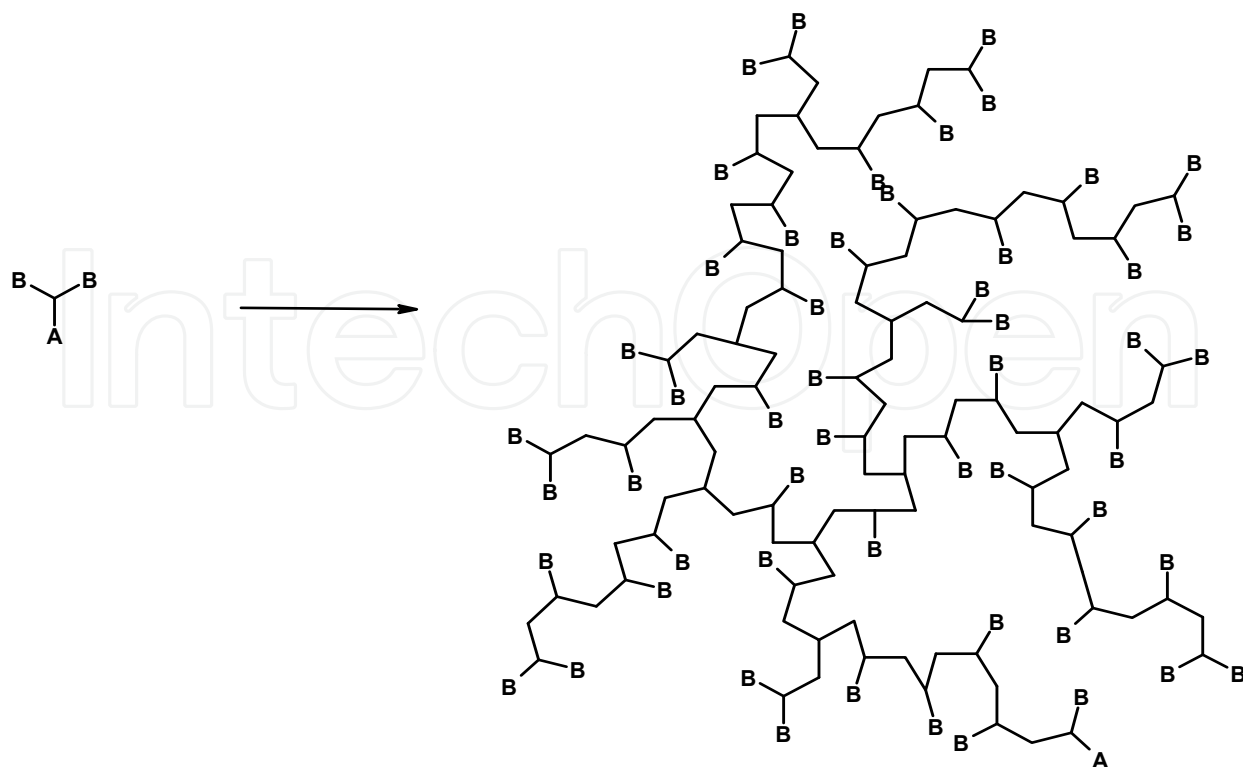


Figure 1. Schematic structure of the hyperbranched polyimide precursor from AB_2 monomer

Polyimides (PI) exhibit very good chemical, mechanical and dielectric stability at temperatures from -150 to 250 °C. These rigid polymers with a high glass transition temperature are mostly used in (micro)electronics, aircraft industry, space exploration and as polymeric separation membranes. Linear polyimides (LPI) are traditionally prepared by the two-step polymerization. The polyimideprecursor, polyamic acid (PAA) (the most often a solution in *N*-methyl-2-pyrrolidone), is prepared from an aromatic dianhydride and an aromatic diamine. This precursor is transformed into a polyimide using thermal or chemical imidization (Figure 2) [5].

It is difficult to prepare hyperbranched polyimides (HBPI) from AB_x monomers due to the high reactivities of A and B groups. Therefore, they are often prepared by the combination of bifunctional (A_2) and trifunctional (B_3) monomers. The ratio of anhydride and amine component determines the kind and the ratio of endgroups. Nevertheless, their synthesis from trifunctional monomers often a rather complex structure requires special and controlled reaction conditions (namely low monomer concentrations, strictly controlled slow addition rates and molar ratios of monomers) to avoid gel formation [4] because it is known that direct polycondensation of A_2 and B_x (x is higher than 2) monomers generally results in three-dimensional product [1]. As such triamines were used, e.g., tris(4-aminophenyl)amine or 1,3,5-tris(4-aminophenoxy)benzene [4].

In the paper [6] it was shown that AB_2 monomer provides HBPI with a higher degree of branching (degree of branching is defined as the ratio of (branching + terminal units)/(branching + terminal + linear units)) and a less level of entanglements in comparison

with the use of A_2 and B_3 monomers (Figure 3) although their chemical structures are very close. A different chain architecture also influenced the viscosity behaviour, glass transition temperature and thermooxidative stability of the products.

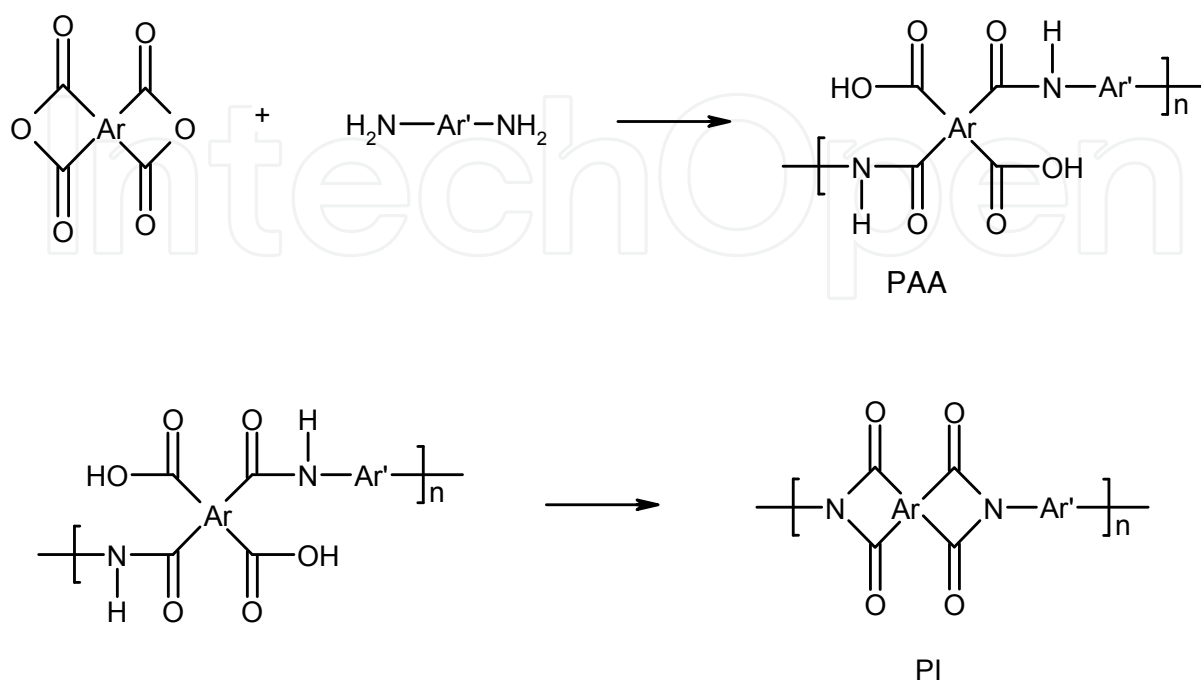


Figure 2. Two-step preparation of polyimides (PI) via a polyamic acid (PAA) precursor

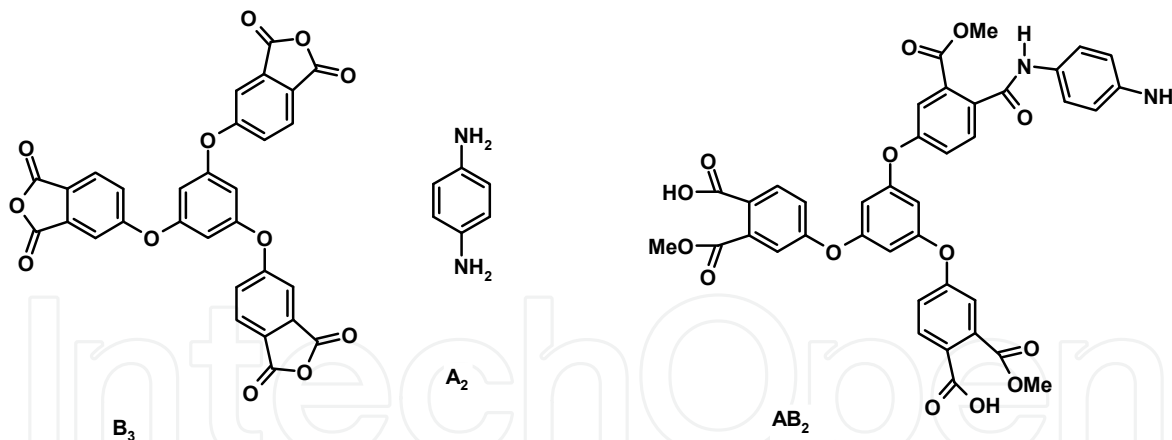


Figure 3. Chemical structure of the monomers A_2 , B_3 and AB_2 used in [6]

Okamoto [7] studied the HBPI synthesis at which the different dianhydrides and tris(4-aminophenyl)amine were used (Figure 4). By using a dianhydride and triamine in molar ratio 1:1 the amine end-capped HBPI and in the ratio 2:1 the anhydride end-capped HBPI were formed. The degree of branching of the amine end-capped HBPI was in the range 0.64-0.72 in the dependence on the kind of dianhydride and this value approached 1 for the anhydride terminated HBPI (independently on a dianhydride). HBPI prepared from 4,4'-(hexafluoroisopropylidene)diphthalic anhydride (Figure 4 a) and tris(4-aminophenyl)amine in their molar ratio 1:1, showed a weight average molar mass $37000 \text{ g}\cdot\text{mol}^{-1}$ and polydispersity

(non-uniformity) 5.8 and the product based on 3,3',4,4'-diphenylsulfonetetracarboxylic dianhydride (Figure 4 b)) and tris(4-aminophenyl)amine in their molar ratio 2:1 150000 g.mol⁻¹ and a very high polydispersity 18.

The difficulties with the formation of a three-dimensional product were not observed if 2,4,6-triaminopyrimidine (Figure 5) was employed as a monomer for the preparation of HBPI probably due to different reactivities of amino groups in the position 2 and positions 4 and 6 [8]. But, as a consequence of it, a less regular HBPI structure is expectable.

The application tests of hyperbranched polymers have namely focused on their employment as non-linear optical polymers, polymer electrolytes, biomaterials, supramolecular components (nanomaterials), photolithographic materials, coatings, modifiers and additives and polymeric membranes so far [3].

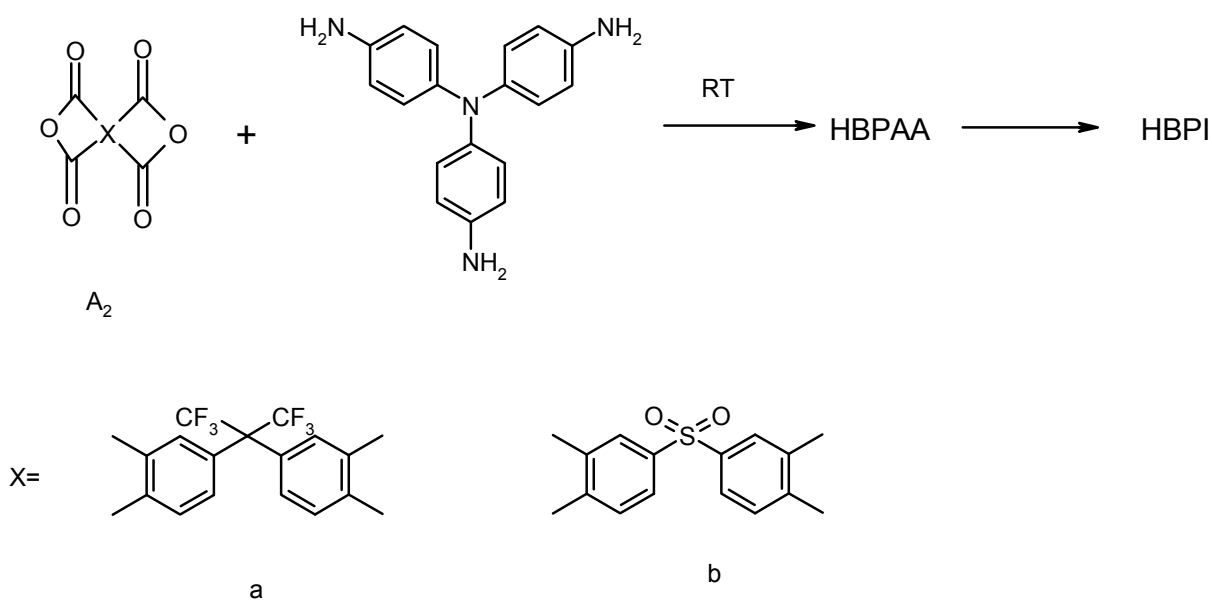


Figure 4. HBPI synthesis from tris(4-aminophenyl)amine and different dianhydrides [7]

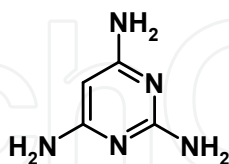


Figure 5. Chemical structure of 2,4,6-triaminopyrimidine

Membrane separation processes belong to a relatively new type of mass-separation techniques. They have been tested or even applied in various technological processes, e.g., of chemical and food industries. Membrane processes could be used, e.g., instead of a cryogenic distillation of air for the production oxygen and nitrogen [9]. Their importance increases also in environmental technologies reducing or eliminating emissions, wastes and pollutants in air and water. Inorganic membranes have high thermal and chemical stabilities, which make them attractive for separations at high temperatures and in aggressive environments. However, inorganic membranes still have technical limitations

and suffer from problems such as brittleness and lack of surface integrity [10]. On the contrary, polymeric membranes are becoming increasingly important for the separation of gas and liquid mixtures because of their low cost and the ease of their production. But two key technical challenges exist in this field. The first of these challenges is to achieve higher ability to separate mixtures with at least equivalent productivity. The second challenge is to maintain these properties in the presence of complex and aggressive feeds (polymeric membranes are traditionally less stable against chemicals and temperature in comparison with inorganic membranes) [10].

Mass transport through a nonporous polymeric membrane is characterized by permeability, diffusion and solubility coefficients which depend particularly on the nature of both the membrane and the penetrant. A level of the separation depends also on additional factors (e.g. temperature). Generally, the permeability (flux) of membranes with excellent separation properties (selectivity) is usually not very high. For practice it is very important to have membranes with high permeability and with sufficient selectivity, too. The permeability in a polymer depends on the solubility and the diffusivity of the permeating species in that polymer. When there exists a large difference in the solubilities of two species mostly rubbers are taken for separation one of other (for example organic vapours recovery from air). When the difference in solubility is low mostly glassy polymers are used so that the separation is more based on the difference in diffusivity which is also governed by the free volume of polymer [9].

From the point of view of a controllable free volume, hyperbranched polymers are a very attractive candidate to the membranes with convenient transport parameters. It is reported that according to the results of computer simulation there are many accessible cavities of atomic size (or slightly larger) in the rigid hyperbranched polymers [11]. As mentioned above the polymers with overall stability are needed for producing some membranes used in separation technologies. Polyimides are available for this purpose.

Non-porous, flat polyimide membranes show high separation factors (selectivities) in separation of gas mixtures but low permeability both of gases and organic vapours. Very high selectivities organic vapours/gases were reached when non-porous flat membranes based on polyimides crosslinked with polyesters and polyethers were employed [12]. Linear aromatic polyimides were successfully used for separation of gases (hydrogen, helium etc.). Composite membranes, asymmetric membranes and hollow fibre membranes based on polyimides were employed for separation of organic vapours from air [9].

Recently, hyperbranched polyimides were auspiciously tested as polymeric membranes for gas separation [11]. Suzuki [13] monitored gas transport properties of the membranes made of 1,3,5-tris(4-aminophenoxy)benzene (Figure 6) and 4,4'-(hexafluoroisopropylidene)diphthalic anhydride and compared these parameters with those for LPI with a similar chemical composition. The permeability, diffusivity and solubility of the gases were higher in the membranes based on HBPI. It seems that the favourable effect of both the chain character (rigidity, interactions, arrangements, higher free volume) and selective gas sorption (cavities, end-capping groups) contributes to this increase. The O₂/N₂ selectivity reached up to 6.2.

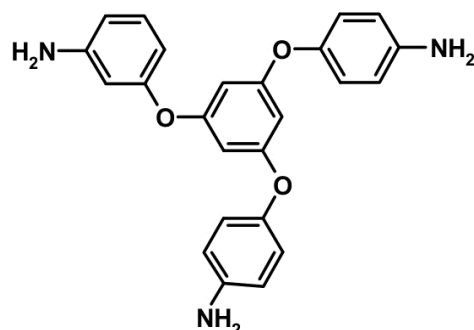


Figure 6. Chemical structure of 1,3,5-tris(4-aminophenoxy)benzene [13]

An influence of the HBPI end-groups on their gas transport properties was studied. The amine-encapped HBPI showed the higher CO₂, N₂ and O₂ permeability coefficients than anhydride-encapped HBPI. The amino groups of HBPI can probably create the stronger interactions with some gases, especially with CO₂ [14]. The introduction of bulky fragments (e.g. via 3,5-di(trifluoromethyl)aniline as the HBPI endgroups) also increased the gas permeabilities but their selectivities were decreased. The membranes prepared from hyperbranched polyimides based on commercially available 4,4',4''-triaminotriphenylmethane were prepared and some of their transport properties tested [15]. The permeability coefficients of hydrogen, carbon dioxide, oxygen, nitrogen and methane in the membrane from HBPI were 2-3.5 times higher than those in the membrane from LPI at comparable selectivities [16]. Fang [11] prepared membranes from HBPI based on tris(4-aminophenyl)amine and a few dianhydrides followed by their crosslinking. Crosslinking was realized by a coupling agent enabling us to link up macromolecules with chemical bonds by using their end-groups. The crosslinking also influenced the transport properties of membranes. The use of coupling agent ethylene glycol diglycidylether resulted in the increase of CO₂ permeability in comparison of that of N₂. On the contrary, by using a more rigid agent terephthalaldehyde the permeabilities of both gases were comparable. The selectivity CO₂/N₂ reached the values up to 32. Crosslinking brings both the reinforcement of resulted polymer structure and the partial loss of compactness of the polymer globular structure.

Nevertheless, studies concerning transport properties of the membranes made of those materials have showed that principal requirements of the membrane technologies on increasing permeability at sufficiently high selectivity are still topical. Generally, it seems that polymeric, non-porous, flat membranes reached their limit.

A promising route to membranes of improved transport characteristics consists in incorporation of inorganic additives with suitable structure (e.g., zeolites, carbon molecular sieves, microporous silica) into polymer matrix [17]. Some of polymer-inorganic composite materials showed much higher permeabilities but similar or even improved selectivity

compared to pure polymer membranes. For example, the polysulfone membranes containing mesoporous silica MCM-41 showed higher gas permeabilities in comparison with that prepared from the net polymer only without a significant decrease in their selectivities [18].

The most commonly used preparation techniques for the fabrication of filled/composite materials are [17]:

1. Solution blending - a polymer is first dissolved in a solvent to form a solution, and then inorganic particles are added into the solution and dispersed by stirring.
2. In situ polymerization - particles are mixed well with organic monomers, and then the monomers are polymerized.
3. Sol-gel - organic monomers, oligomers or polymers and inorganic nanoparticle precursors are mixed together in the solution. The inorganic precursors then hydrolyze and condense into well-dispersed nanoparticles in the polymer matrix.

Polyimides exhibit outstanding dielectric and mechanical properties at elevated temperatures. Nevertheless, relatively high values of water sorption (up to 3-4 wt%) and coefficients of thermal expansion ($5 \times 10^{-5} \text{ K}^{-1}$) impede (micro)electronic applications, e.g., forming stress-free films on silicon substrates. From this point of view silica (SiO_2), that exhibits very low values of water sorption and coefficients of thermal expansion ($5 \times 10^{-7} \text{ K}^{-1}$), would be more suited for (micro)electronic applications but dielectric properties and planarizability are inferior to PI [17]. Combined materials exhibiting favourable properties of both polyimides and silica are therefore in great demand.

From this point of view, the preparation and characterization of materials combining these components appear as highly topical. Therefore, the new mixed matrix materials prepared from HBPI based on the commercially available MTA and mesoporous silica MCM-41 or nanoparticles of silica, whose inorganic and organic phases are linked up by covalent bonds in selected cases, were made and their properties were studied in this work.

2. Experimental

4,4'-Oxydiphthalic anhydride (ODPA) (Figure 7 b) was heated to 170 °C for 5 h in a vacuum before use. 4,4'-Methylenedianiline (MDA) (both Aldrich, Czech Republic) (Figure 7 c) and 4,4',4''-triaminotriphenylmethane (MTA) (Dayang Chemicals, China) (Figure 7 a) were used as received. Mesoporous silica MCM-41 (M- SiO_2) having a pore size 2.5-3 nm and nanosilica (N- SiO_2) having a particle size 10-20 nm and surface area 160 $\text{m}^2 \text{ g}^{-1}$ (both Aldrich) were heated to 120 °C for 3 h in an oven before use. 3-Glycidoxypropyltrimethoxysilane (GPTMS) (Aldrich) was used as received.

1- Methyl-2-pyrrolidone (NMP; Merck, Czech Republic) was distilled under vacuum over phosphorus pentoxide, and stored in an inert atmosphere. Gases in the gas cylinders (Siad, Czech Republic) were used as received (nitrogen 99.99 vol%, oxygen 99.5 vol%, methane 99.0 vol%, carbon dioxide 99.0 vol%, hydrogen 99.90 vol%).

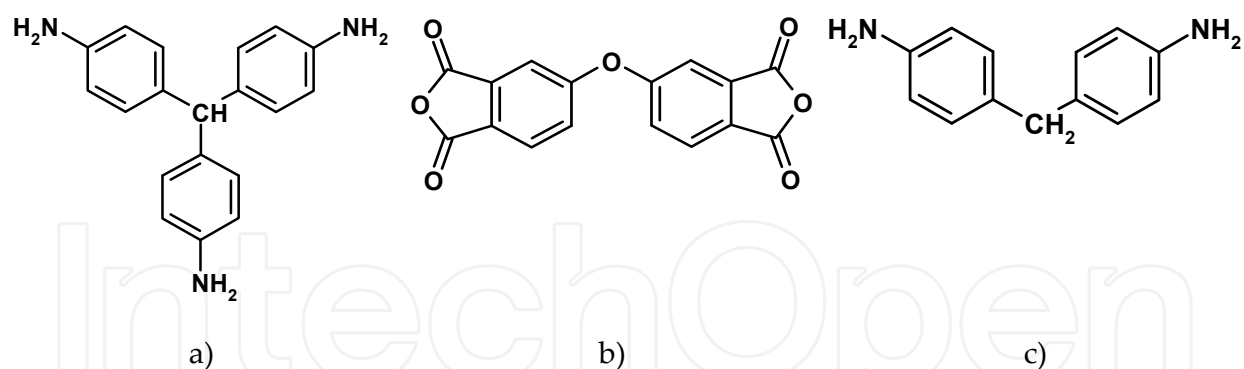


Figure 7. Chemical structure of a) 4,4',4''-triaminotriphenylmethane, b) 4,4'-oxydiphthalic anhydride and c) 4,4'-methylenedianiline

HBPAA and LPAA were prepared in a two necked flask equipped with a magnetic stirrer and a nitrogen inlet/outlet. At room temperature ODPA solution in NMP was added dropwise to a solution of MTA or MDA in NMP. This reaction mixture was then stirred at room temperature for 24 h. The general procedure for the preparation of amine end-capped HBPAA based on ODPA and MTA [HBPAA(ODPA-MTA)11] is followed: At room temperature, a solution of 4.973 g (0.016 mol) ODPA in 65 ml of NMP was added dropwise to a solution of 4.562 g (0.016 mol) of MTA in 86 ml of NMP for approximately 1 h. This reaction mixture was then stirred at room temperature for 24 h.

A mixture of HBPAA with M-SiO₂ or N-SiO₂ was prepared by adding the calculated amount of silica particles to the 4 wt% solution of polyimide precursor in NMP under stirring with a magnetically driven stirrer. The preparation of mixture (suspension) under stirring proceeded for 12 h. Some of M-SiO₂ and N-SiO₂ were reacted with GPTMS before use.

For the preparation of membranes based on HBPI or LPI or HBPI and silica a solution of either HBPAA or LPAA or a suspension of silica in HBPAA solution were spread onto a glass substrate (treated with chlorotrimethylsilane). The resulting thin layer was kept at 60 °C for 12 h, 100 °C for 1h, 150 °C for 1 h, 200 °C for 2 h and 250 °C for 1 h. The thickness of the self-standing films obtained was about 50 - 100 μm.

¹H NMR spectra were taken on Bruker Avance DRX 500 at 500 MHz in d₆-dimethylsulfoxide. IR spectra were recorded on a Nicolet 740 spectrometer using a reflective mode. Thermogravimetric measurements (TGA) were performed in air using a TG-750 Stanton-Redcroft. The glass transition temperatures were found by using a dynamic mechanical analysis (an instrument DMA DX04T (RMI, Bohdanec, Czech Republic) operating at 1 Hz and in the temperature range 25-400 °C with a temperature gradient 3 °C min⁻¹). Scanning electron microscopy was made by using a microscope Jeol JSM-5500 LV. The material cross section areas were covered by a deposited platinum layer prior to measurement. The following procedure was used to test the chemical resistance of the materials in the NMP, as well as in methanol and toluene: each film was dried at 100 °C for 3 h, weighed, and immersed in an appropriate solvent. After 35 days the weight change was determined. The kinematic viscosities of the HBPAA and LPAA solutions were measured

using a capillary viscometer at 20 °C, and their intrinsic viscosities measured in NMP at 25 °C. The permeation measurements were conducted using the self-developed manometric integral apparatus, the detailed description of which is given in [16]. The values of permeation coefficients vary within the accuracy of measurement up to 20% if experiments are repeated (especially in the case of methane due to its extremely low permeation).

3. Results and discussion

In this work, the commercially available monomers - bifunctional 4,4'-oxydiphthalic anhydride (ODPA) and trifunctional 4,4',4''-triaminotriphenylmethane (MTA) - were used for the hyperbranched polyimide (HBPI) preparation. Based on its composition the final hyperbranched polyimide (HBPI) is designated as HBPI(ODPA-MTA) or as the case may be with an additional specification of the monomer molar ratio [e.g. HBPI(ODPA-MTA)₁₁ if ODPA and MTA were used in the molar ratio 1:1]. The use of the commercially available monomers is reasonable from the point of view of a shift to the larger (industrial) scale.

Due to the MTA structure the identical reactivity of its three amino groups is expectable which is one of the basic requirements of the regular branched polymeric structure [8]. In the case of ODPA it was shown that the presence of the ether bridge (-O-) decreases the glass transition temperature of the final PI in comparison with those cases where different dianhydrides were employed [15]. The lower rigidity of polymer chains can favourably influence the preparation of self-standing films. Their successful formation is important for the evaluation of the thermo-mechanical and transport properties of these materials. Knowledge of these properties is substantial for making conclusions concerning potential applications. For the better evaluation of the specific HBPI(ODPA-MTA) properties the linear polyimide (LPI) based on ODPA and bifunctional amine 4,4'-methylenediamine (MDA) [LPI(ODPA-MDA)₁₁] in their molar ratio 1:1 was also prepared and characterized. 1-Methyl-2-pyrrolidone (NMP) was used as a solvent. It dissolves both monomers and polyimide precursors (PAA). Due to its hygroscopic character it was distilled in vacuum in the presence of a phosphorus pentoxide.

The MTA quality (purity) was determined by using ¹H NMR (Figure 8). It is obvious a very good relation between the integral intensity of signals belonging to the aromatic protons (6.7-6.4 ppm) and those to the protons of amino groups (4.87-4.82 ppm). Unfortunately, the integration of the signal of methine (-CH-) group is not possible due to its coincidence with another signal.

The two-step preparation via an intermediate (HBPA or LPAA) was chosen for the preparation both HBPI (Figure 9) and LPI [5]. Taking into consideration the gel (crosslinked structure) formation at definite reaction extent during the reaction of a bifunctional and a trifunctional monomer [15], our attention was also devoted to the choice of optimal reaction conditions of the HBPI(ODPA-MTA) preparation. The maximal monomer concentrations in NMP and the way of their combination were especially found. The dianhydride solution was added drop-to-drop to the diamine solution. This monomer order also decreases a probability of the dianhydride hydrolysis during an intermediate preparation.

Two monomer molar ratios were used for the HBPA preparation. The ODP A:TMA ratio 1:1 gave an amine end-capped HBPA and that 2:1 an anhydride end-capped HBPA (Figure 10). The maximally available HBPA concentrations – to avoid a gel formation – varied to some extent in the dependence on their character (Table 1) [15]. The higher maximal concentration for the amine end-capped HBPA (0,2 mol.l⁻¹) in comparison with that terminated with anhydride groups (0,075 mol.l⁻¹) is also reported in [7]. The combination of the monomer solutions at their molar concentration ratio 1:1 was also used for the preparation of LPAA.

PAA specification	PAA content ^a (wt%)	N ^b (m ² .s ⁻¹)	[η] ^c (ml.g ⁻¹)
HBPA(ODPA-MTA)11	4	3.17x10 ⁻⁵	54
HBPA(ODPA-MTA)21	1	2.23x10 ⁻⁶	36
LPAA(ODPA-MDA)11	4 ^d	2.83x10 ⁻⁵	28

^amaximal concentration of HBPA in the final solution without an immediate gel formation

^bkinematic viscosity of the solution at 20 °C

^climiting viscosity number (intrinsic viscosity) of HBPA (in 0.075 mol.l⁻¹ LiCl in NMP at 25 °C)

^dcontent of solids was chosen

Table 1. Polyamic acids (PAA) and their characterization

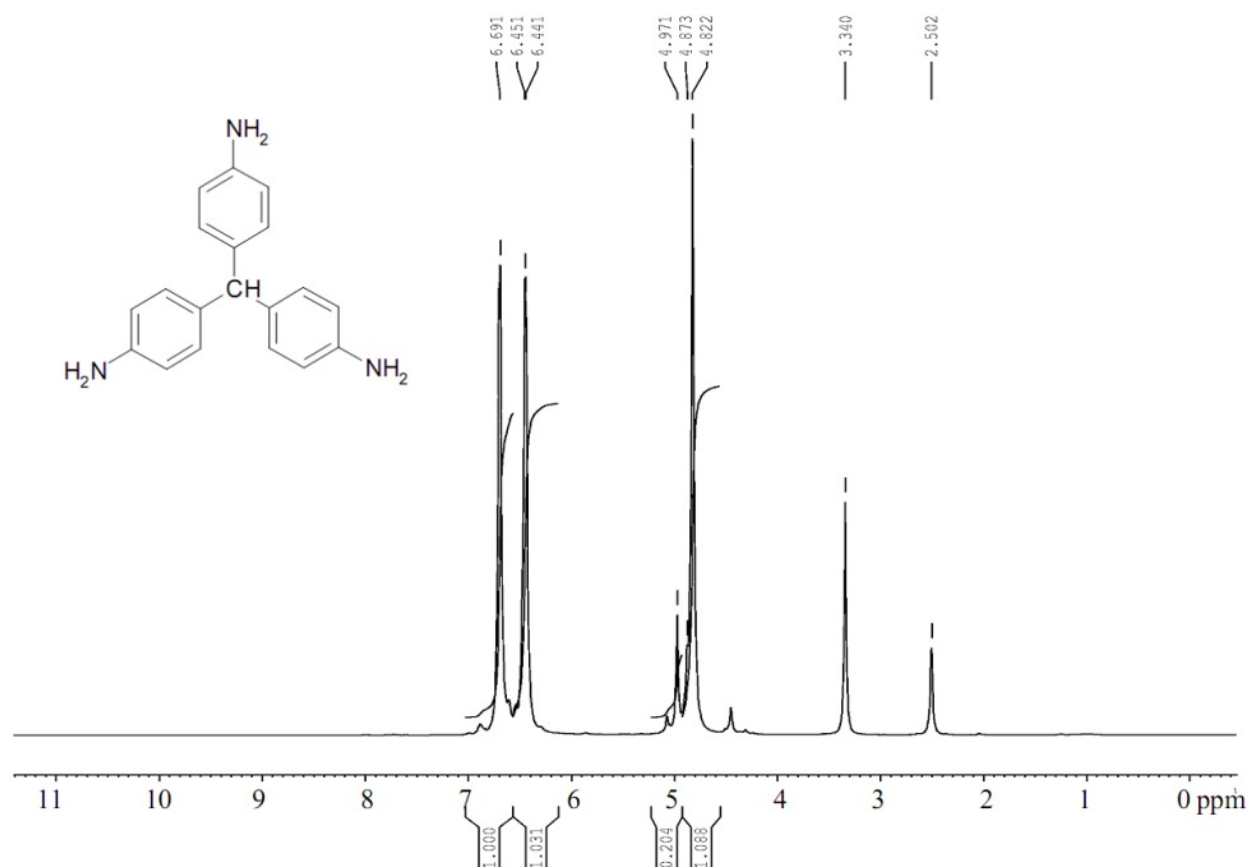


Figure 8. ¹H NMR spectrum of MTA

In the case of LPAA(ODPA-MDA)11 the maximal solution concentration is not a limiting factor of their preparation and it was chosen 4 wt% in agreement with that for HBPA(ODPA-MTA)11. Actually, HBPA(ODPA-MTA)11 was only employed in further work. The final product HBPI(ODPA-MTA)11 provides self-standing films with a good mechanical stability in contrast to HBPI(ODPA-MTA)21. In addition to it, amino end-groups served as reactive sites for linking up the polyimide matrix with silica particles by using the coupling agent 3- glycidyloxypropyltrimethoxysilane.

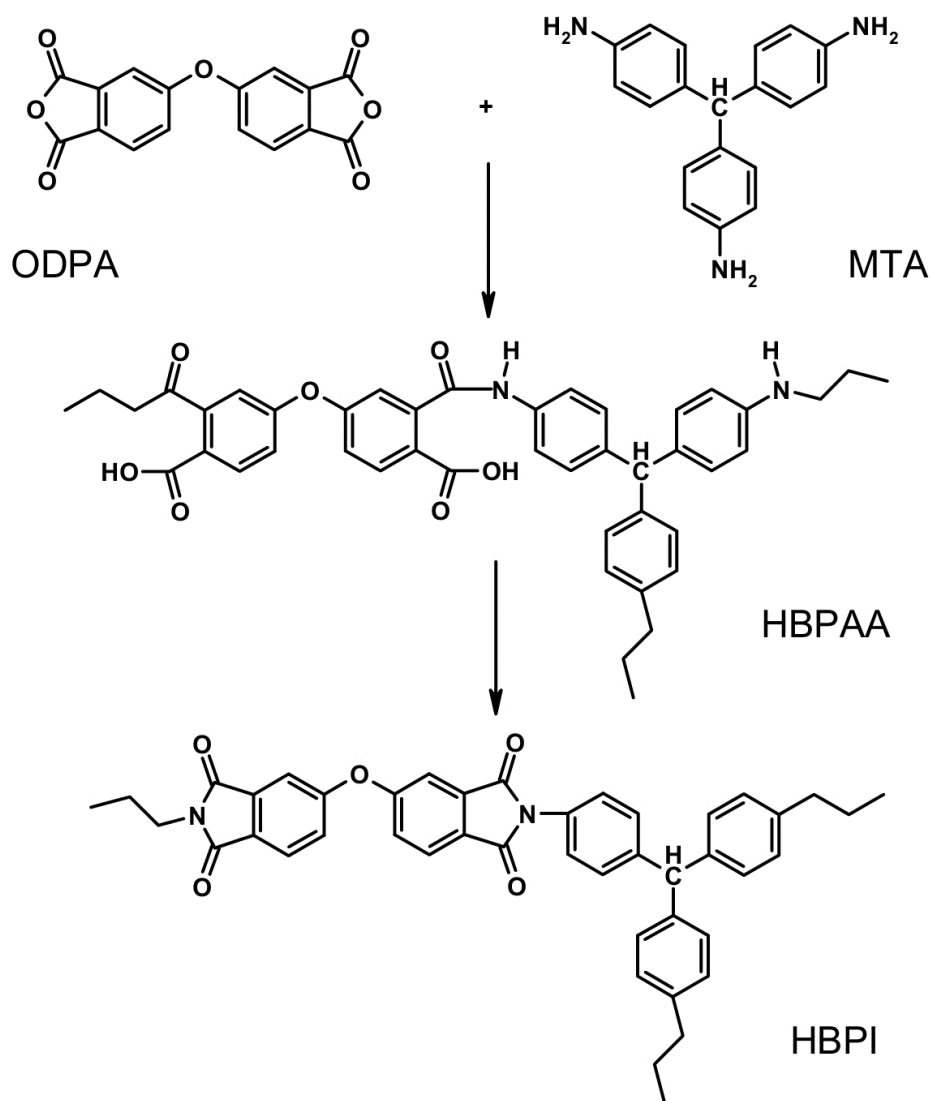


Figure 9. Two-step preparation of HBPI(ODPA-MTA)

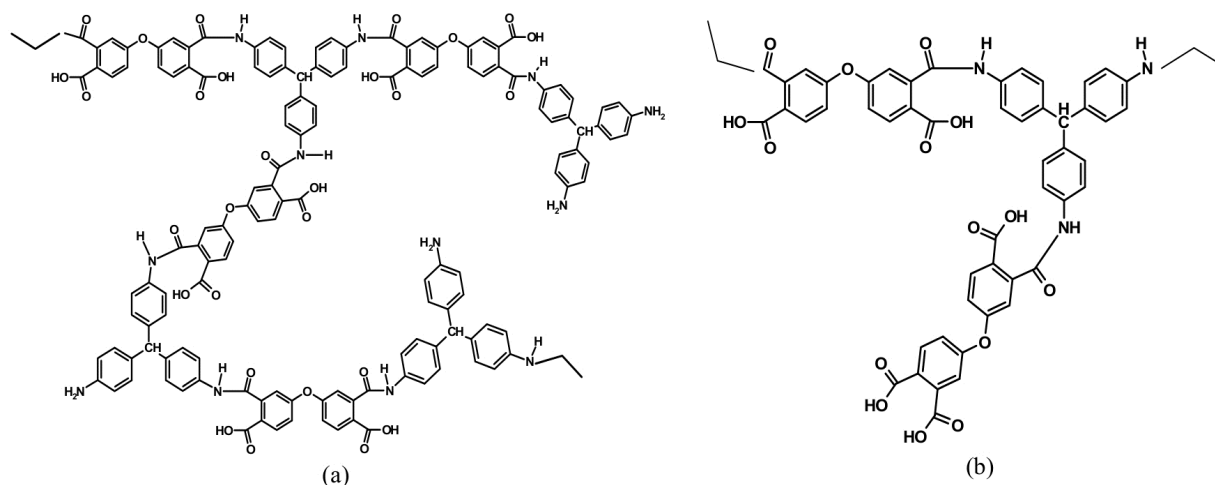


Figure 10. Chemical structure of a) amine and b) anhydride terminated HBPAAs(ODPA-MTA)

The kinematic viscosities of the PAA solutions of a defined (given) concentration and limiting viscosity numbers (intrinsic viscosities) of PAA are also given in Table 1. It is obvious that kinematic viscosities are proportional to the solution concentrations (cf. 4 wt%) solution of HBPAAs(ODPA-MTA)11 and 1 wt% solution of HBPAAs(ODPA-MTA)21. But it is not a significant difference between the solution of hyperbranched [HBPAAs(ODPA-MTA)11] and linear [LPAA(ODPA-MDA)11] PAA having the same theoretical solution concentration (4 wt%). Nevertheless, it was found that the kinematic viscosities of these solutions changes to a certain degree with their storage (i.e. between its preparation and analysis). For example, the kinematic viscosity of HBPAAs(ODPA-MTA)11 was changed about of 10% during 50 days. Therefore, the solutions were processed (transformed to the corresponding polyimides (PI)) immediately after their preparation. It is expected that both HBPAAs formation and degradation (hydrolysis) reactions occur (take place) simultaneously [5]. Limiting viscosity number $[\eta]$ serves as an indicator of a viscosity average molecular mass M_v . It can be calculated for the given system a polymer – solvent at a defined temperature by using a Mark –Houwink equation $[\eta] = K \cdot M_v^a$, where a , K are parameters. These parameters are tabulated for common polymers, but for PI exceptionally only. In addition to it, majority of PI is not soluble and therefore polyimide precursors can only be characterized by viscometry. Limiting viscosity number is determined from the linear dependence of the reduced viscosity on solution concentration as an extrapolated value at the zero concentration. To obtain the linear dependence a polyelectrolytic effect must be avoided. For this purpose, lithium chloride in the concentration of 0.075 mol.l^{-1} was added into NMP, which was used as the solvent for viscometry measurements [15]. From Table 1 it is obvious, that $[\eta]$ of HBPAAs(ODPA-MTA)11 (i.e. amine end-capped HBPAAs) is about 50% higher than that for HBPAAs(ODPA-MTA)21 (i.e. anhydride end-capped HBPAAs).

This difference in $[\eta]$ should also be given by the different degree of branching HBPAAs(ODPA-MTA)11 and HBPAAs(ODPA-MTA)21. Degree of branching is determined from the fraction of dendritic, linear and terminal units included in the given polymer structure (see above). It is necessary to find a group of atoms occurring in all these structures

and monitor it by using a suitable instrumental technique. In the case HBPA(ODPA-MTA)₁₁ and HBPA(ODPA-MTA)₂₁ the position of methine group (-CH-) coming from MTA was monitored in ¹H NMR spectra of given HBPA. The values of shifts for the dendritic, linear and terminal units were found by helping of the ¹H NMR analysis of model reactions of MTA and phthalic anhydride in the molar ratio 1:1, 1:2 and 1:3 and p-toluidine (4-aminotoluene) with phthalic anhydride in the molar ratio 1:1. The model reactions were carried out in deuterated dimethylsulfoxide to avoid the isolation and re-dissolution of these products for NMR analyses.

In the ¹H NMR spectrum of MTA (Figure 8) there are the signals corresponding to the amino group protons (4.82 ppm) and to the methine group proton (4.97 ppm) very close each other and their integration is accompanied with problems. In the spectra of model compounds (i.e. MTA with phthalic anhydride) the signals of methine protons shift to 5 - 6 ppm and they are separated from those of unreacted amino groups at 6.5 - 6.7 ppm markedly (as seen in a model reaction of p-toluidine with phthalic anhydride also). From the ratio among signals in the 5 - 6 ppm range the conclusion was made that the signal with the highest shift belongs to the linear units and with the lowest shift to the terminal units. ¹H NMR spectra of HBPA(ODPA-MTA)₁₁ and HBPA(ODPA-MTA)₂₁ are collected in Figure 11. The broad signal at about 13 ppm belongs to the protons of carboxylic groups, the signal at 10.4 ppm to protons of amide groups, at 8 - 7 ppm to aromatic protons. The degree of branching was determined as ca. 0.7 for HBPA(ODPA-MTA)₁₁ and 0.9 for HBPA(ODPA-MTA)₂₁.

The transformation of HBPA or LPAA into corresponding final products was conducted by using of a thermal imidization in solid phase. This technique is commonly employed for the preparation of insoluble PI. The products are often the layers having a thickness in the range of 1-100 μm. The thickness of the films in this study was about 50 μm. The layer (with a thickness about 1 mm) of the HBPA or LPAA solution was cast on a glass substrate. A majority of the solvent escaped during heating it in the oven in (circulating) air atmosphere at 60 °C. Then, the temperature was gradually increased, finally to 230 - 250 °C, to reach a full imidization and avoid a formation of holes and bubbles in the film (Figure 12). As already mentioned, the mechanical stability of HBPI(ODPA-MTA)₂₁, prepared from 1 wt% solution of (HBPA(ODPA-MTA)₂₁ (see Table 1), was very poor and it was not used in further studies.

The level of transformation of HBPA(ODPA-MTA)₁₁ and LPAA(ODPA-MDA)₁₁ into corresponding PI was analyzed by IR spectroscopy (Figure 13). The absorption bands at about 1780 and 1720 cm⁻¹ (symmetric and asymmetric stretching of the ring carbonyl groups), together with the band at 1380 cm⁻¹ (stretching of the ring C-N bond), are distinct in the spectrum of PI and characterize the formation of imide structures. The absence of the band at 1680 cm⁻¹ [amide group of polyamic acid - see the IR spectrum of HBPA(ODPA-MTA)₁₁] supports our notion that thermal treatment leads to almost complete imidization. The spectrum of the HBPI(ODPA-MTA)₁₁ whose amino end-groups were reacted with phthalic anhydride THBPI(ODPA-MTA) was also taken. This material was prepared to judge the influence of the amino end-groups on its behaviour. The band of terminal amino

groups at ca 1620 cm^{-1} is overlapped in the spectra of both corresponding HBPAA and HBPI. Nevertheless, it is distinct in the IR spectra of model reactions of TMA with phthalic anhydride (see above). Its intensity is proportional to the molar ratio of these components (Figure 14).

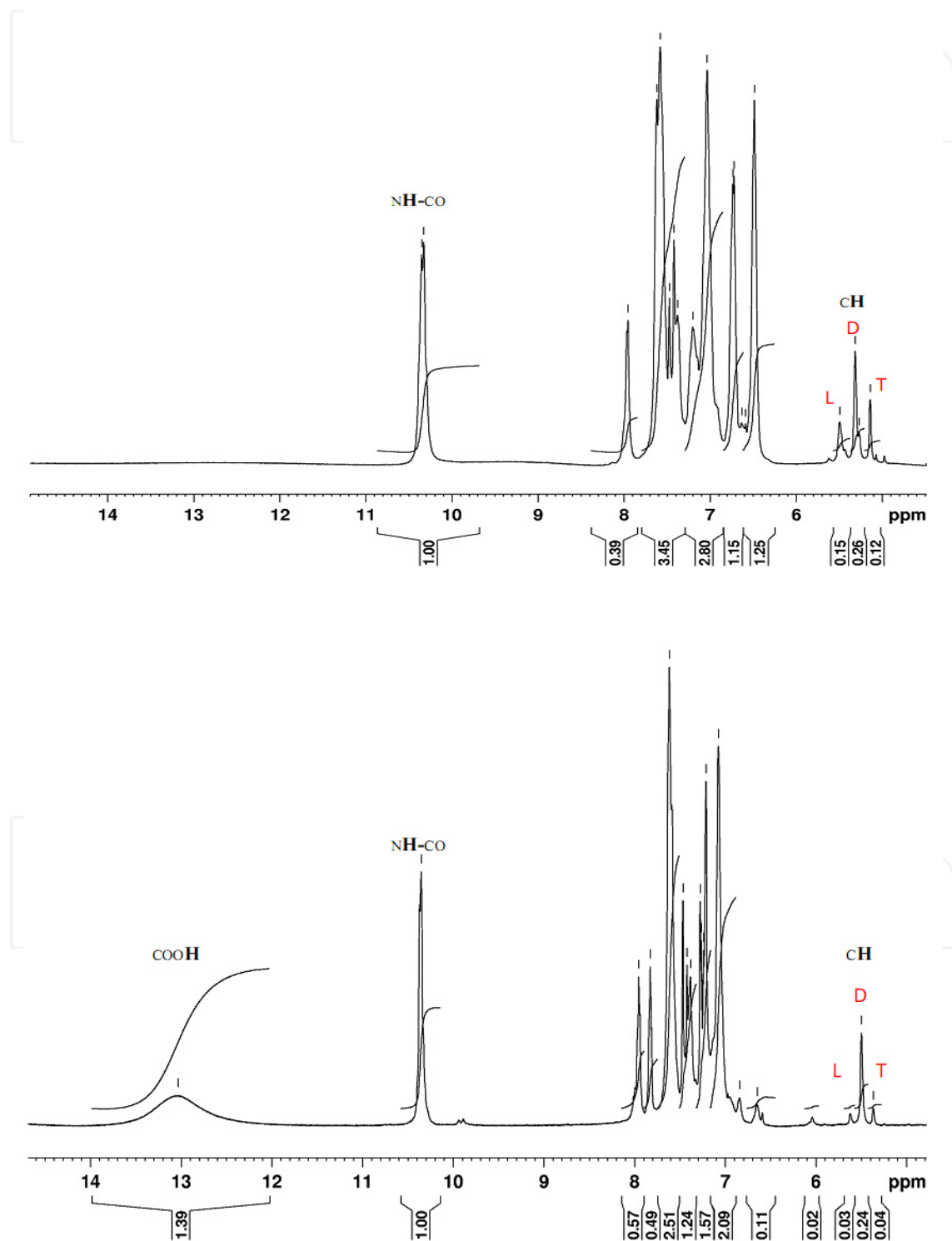


Figure 11. ^1H NMR spectra of (top) HBPAA(ODPA-MTA)11 and (bottom) HBPAA(ODPA-MTA)21

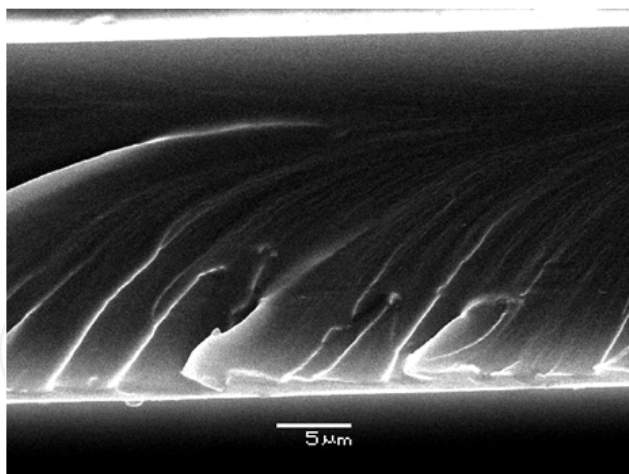


Figure 12. SEM photograph of HBPI(ODPA-MTA)11

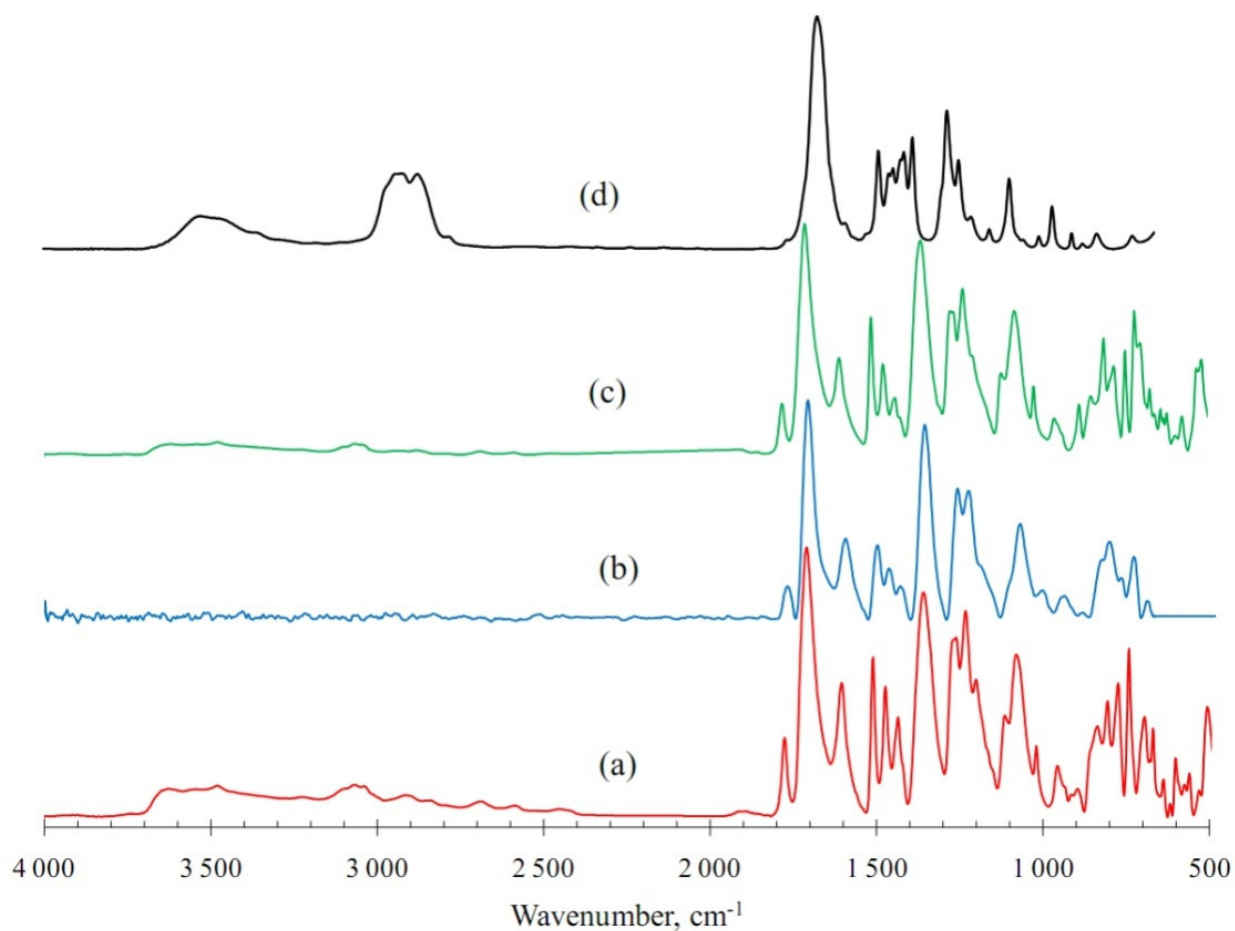


Figure 13. IR spectra of a) LPI(ODPA-MDA)11, b) HBPI(ODPA-MTA)11, c) THBPI(ODPA-MTA)11, d) HBPA(ODPA-MTA)11

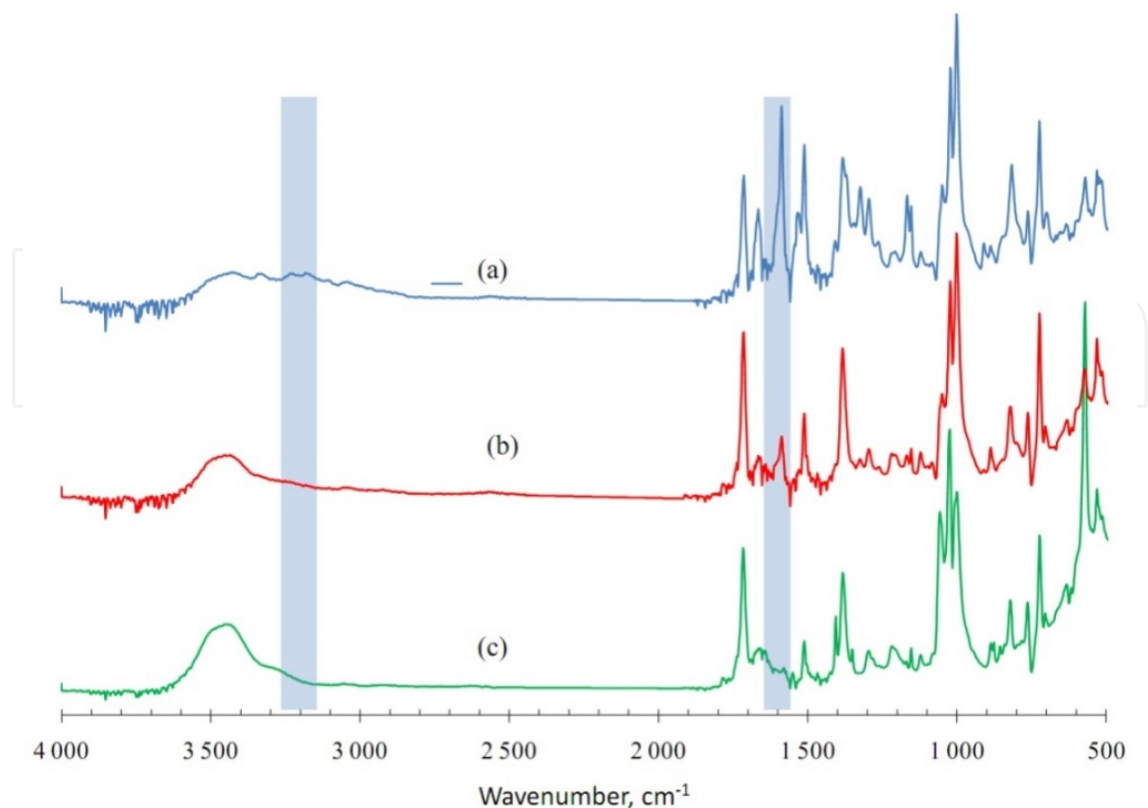


Figure 14. IR spectra of model compounds prepared from MTA and phthalic anhydride in molar ratio (a) 1:1, (b) 1:2 and (3) 1:3

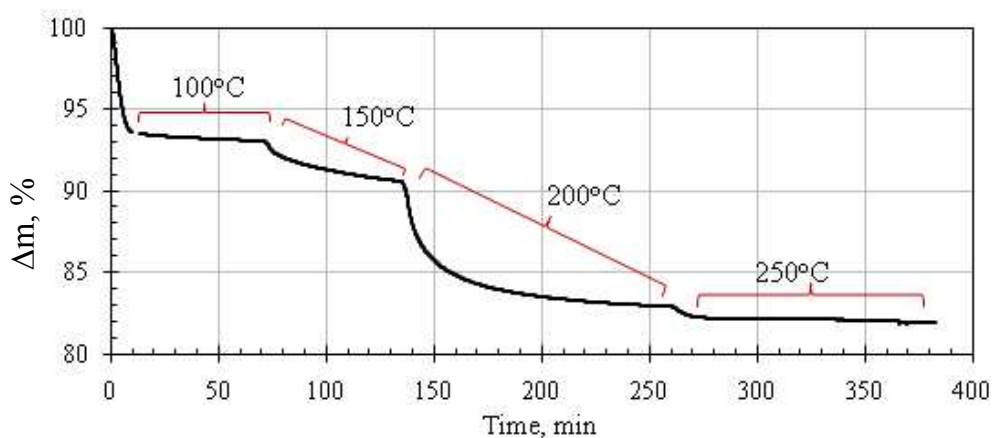


Figure 15. TGA record simulating the HBPA(ODPA-MTA)11 imidization

The choice of the final imidization temperature is limited on the one side by practically full imidization and on the other side by the request of the stability of the product under these conditions. To support the second request, HBPA(ODPA-MTA)11 was processed by using a thermogravimetric analysis simulating the imidization proces. It is obvious from Figure 15 that the product is stable (a weight loss is practically unchanged) at 250 °C.

Materials HBPI(ODPA-MTA)11 and LPI(ODPA-MDA)11 were analyzed by using a dynamic-mechanical analysis (DMA). The records ($\tan \delta$) vs temperature of both materials, which are very different, are shown in Figure 16 a,b.

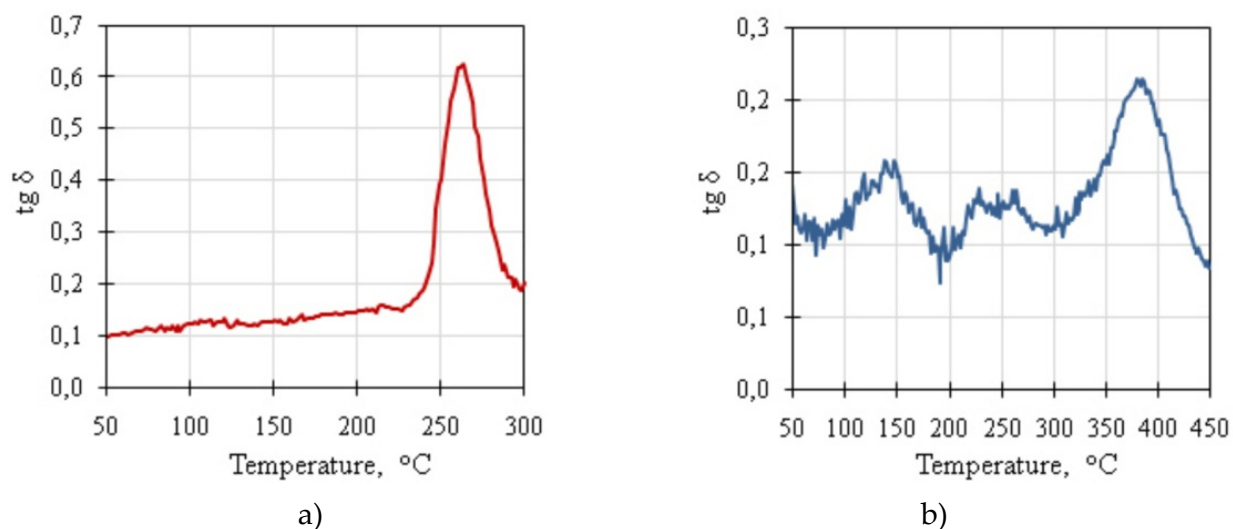


Figure 16. DMA records of a) LPI(ODPA-MDA)11 and b) HBPI(ODPA-MTA)11

DMA record of LPI(ODPA-MDA)11 provides one rather broad band with a maximum at 263 °C corresponding to its glass transition temperature. On the other hand, HBPI(ODPA-MTA)11 record is very complicated. It is created by a few partly overlapped bands in the temperature region from 50 to 400 °C. The band at above 250 °C is bringing by a linear portion and that above 370 °C by a hyperbranched portion of the product. The accuracy of these DMA measurements is about ± 5 °C.

To evaluate activation energies of thermooxidative decomposition the materials HBPI(ODPA-MTA)11, THBPI(ODPA-MTA)11 and LPI(ODPA-MDA)11 were analyzed by a thermogravimetric analysis using heating rates 2,5; 5; 10 and 15 °C.min⁻¹. The obtained dependences are collected in Figure 17 a, b.

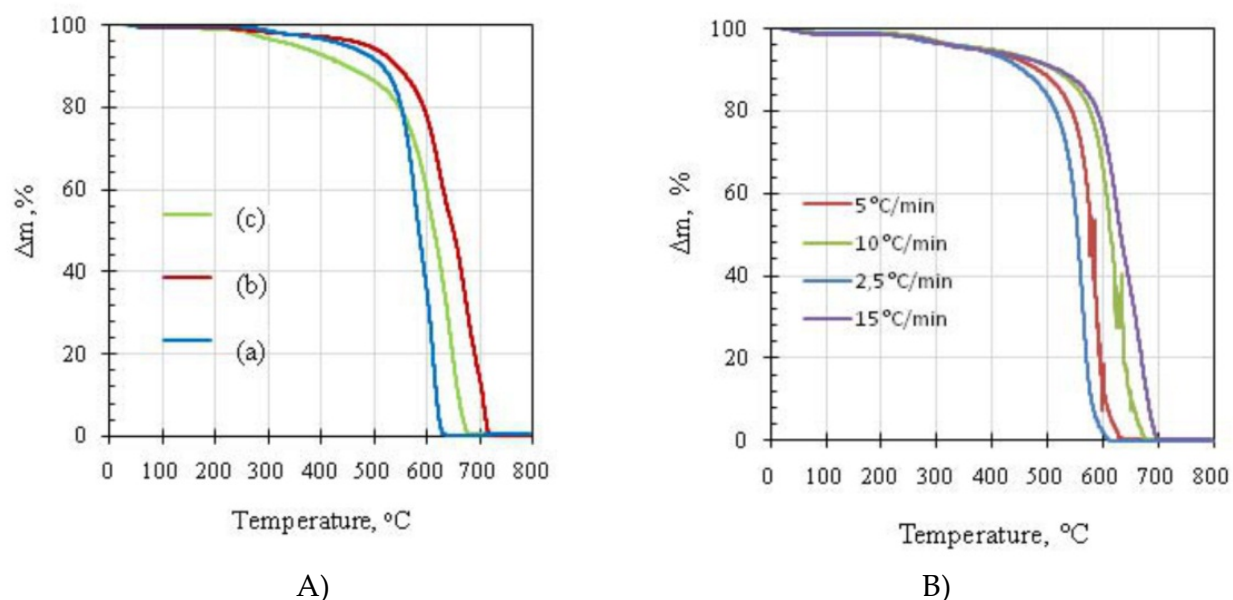


Figure 17. TGA records in air atmosphere of A) HBPI(ODPA-MTA)11 (a), THBPI(ODPA-MTA)11 (c), LPI(ODPA-MDA)11(b) at heating rate 10 °C.min⁻¹; B) HBPI(ODPA-MTA)11 at heating rates 2,5; 5; 10 and 15 °C.min⁻¹

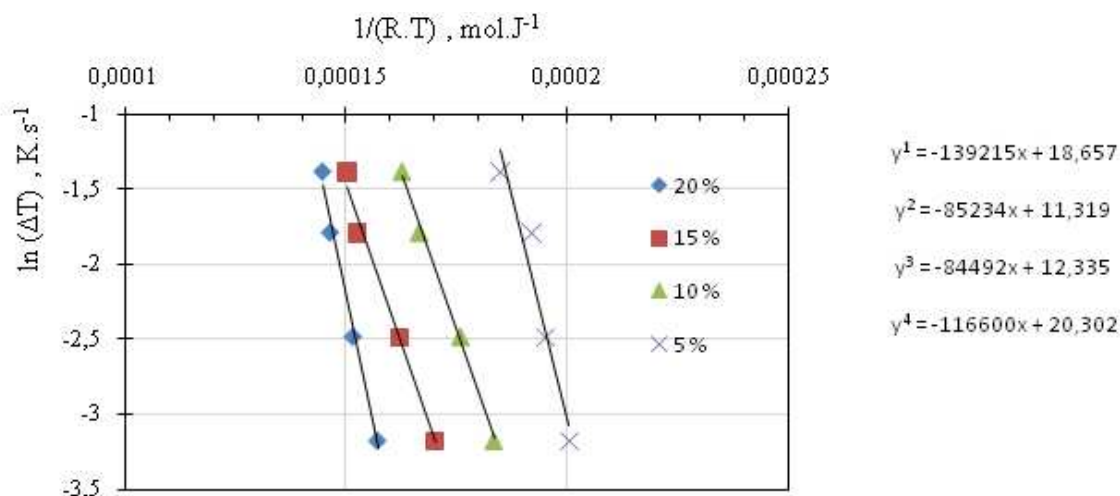


Figure 18. Graphical evaluation of the activation energies of different levels (from 5 to 20 wt%) of the thermooxidative decomposition of THBPI(ODPA-MTA)11 (regression equations are also given in this figure).

Material	E_a (kJ mol ⁻¹)
HBPI(ODPA-MTA)11	127
THBPI(ODPA-MTA)11	106
LPI(ODPA-	184

Table 2. Activation energies of thermooxidative decomposition of HBPI(ODPA-MTA)11, THBPI(ODPA-MTA)11 and LPI(ODPA-MDA)11

The values of temperature corresponding to the weight loss from 5 to 20 wt% were used for the evaluation of activation energy of thermooxidative decomposition E_a by using an Arrhenius equation

$$\ln(k) = \ln(A) - E_a \cdot \frac{1}{R \cdot T},$$

where k is a heating rate, R is a gas constant, T is an absolute temperature.

The activation energies for the weight losses from 5 to 20 wt% were determined from the dependence of $\ln k$ on reciprocal value T ($1/T$). It is shown for THBPI(ODPA-MTA)11 in Figure 18. The average values of activation energies in the region 5 – 20 % are collected in Table 2.

The E_a of HBPI(ODPA-MTA)11 is about 30 % lower than that of LPI(ODPA-MDA)11 and the blockage of amino end-groups decreases the E_a of THBI(ODPA-MTA)11 in comparison with HBPI(ODPA-MTA)11 about 20 kJ mol⁻¹. The order of these values supports the relation of the temperatures corresponding to, e.g., 10 wt% loss in air at a heating rate 10 °C.min⁻¹ (544 °C for LPI(ODPA-MDA)11, 513 °C for HBPI(ODPA-MTA)11 and 448 °C for THBPI(ODPA-MTA)11 (also see Figure 17 a).

It is clear that the blockage of amino end-groups of HBPI(ODPA-MTA)11 worsens its thermooxidative stability. It is probably a consequence of a non-existence of interactions of these groups [19].

The deeper information concerning a thermooxidative decomposition was obtained by using thermogravimetric analysis combined with an IR analysis of degradation products. It is obvious from the IR spectra taken at 670 °C (Figure 19) that the main degradation product is carbon dioxide (band at 2350 cm^{-1}). The carbon monoxide (ca 2150 cm^{-1}), water (3500 cm^{-1}) and aromatic fragments (1500 cm^{-1}) were also identified in the spectra.

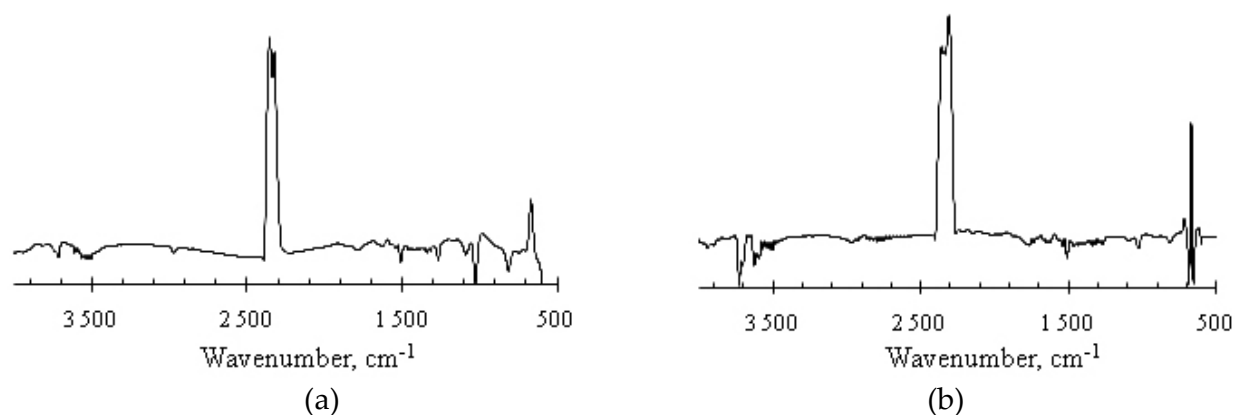


Figure 19. IR spectra of the degradation products of thermooxidation of a) HBPI(ODPA-MTA)11, b) LPI(ODPA-MDA)11 at 670 °C

Both the HBPI and LPI were not soluble in NMP, toluene and methanol. It means that the hyperbranched architecture of polymer chains does not contribute to the solubility. The permeability coefficients of hydrogen, oxygen, nitrogen and methane in the membrane prepared from HBPI were ca 2 and of carbon dioxide 3.7 times higher than those in the membrane from LPI at comparable selectivities (e.g., selectivity oxygen/nitrogen about 6) [16].

As an additive to the hyperbranched polyimide matrix the silica was chosen. It has a lot of favourable properties and it is available in a lot forms. These forms were chosen with a view of improving permeability/selectivity relation of the membranes made of these materials. Compact (non-porous) additives generally decrease a gas permeability due to their behaviour as a barrier for a gas molecule trajectory [17]. Therefore, the mesoporous silica (M-SiO₂) and non-porous nanosilica (N-SiO₂) were chosen for this work. M-SiO₂ with a particle size about 1 μm shows a pore diameter about 2.5 nm, i.e. the diameter larger than that of gases whose permeability was tested in this work (0.29 nm for H₂, 0.33nm for CO₂, 0.35 nm for O₂, 0.36 nm for N₂ and 0.38 nm for CH₄ [18]). In the case of N-SiO₂ with a particle size about 15 nm, a large interfacial area, having different properties than both polyimide matrix and silica, can be expected. By using a titrimetric determination (weakly acidic Si-OH groups were treated with NaOH and an unreacted portion of NaOH was titrated with HCl) the silanol group concentrations (Si-OH) 1.3 and 0.3 $\text{mmol}\cdot\text{g}^{-1}$ were found for M-SiO₂ and N-SiO₂, respectively. The higher Si-OH concentration in the case of M-SiO₂ corresponds with its larger surface in comparison with N-SiO₂.

In the selected cases (samples), the organic and inorganic phases were bound by the covalent bonds by using a coupling agent 3- glycidyloxypropyltrimethoxysilane (GPTMS). Its epoxy groups react with amino end-groups of HBPI(ODPA-MTA)11 (Figure 20) and its alkoxy groups (after their hydrolysis to hydroxyl groups) with the surface hydroxyl groups

of silica (it is schematically shown in Figure 21). The consequence of covalently bound phases could be also a better distribution of the silica particles in a polymer matrix [17,20].

The IR spectra of the non-functionalized and GPTMS functionalized M-SiO₂ are shown in Figure 22. The bands at about 1100 cm⁻¹ correspond with Si-O-Si atom arrangement. The completeness of functionalization is supported by the disappearing of the broad band at 3400 cm⁻¹ corresponding to silanol groups (Si-OH).

The calculated amounts of unmodified or modified silicas were mixed with HBPA(O-DPA-MTA)11 to obtain the mixtures with 5 – 20 wt% content of additive. The layers of these mixtures (with a thickness about 1 mm) on a substrate were gradually heated, finally at 250 °C for 2 h. The IR spectra of HBPI(O-DPA-MTA)11 containing theoretically 16 wt% of M-SiO₂ or N-SiO₂ are shown in Figure 23. In addition to the peaks characterizing polyimide moieties (see above) the broader bands with a maximum about 1100 cm⁻¹ are present. It confirms that silicas were built in the polyimide matrix.

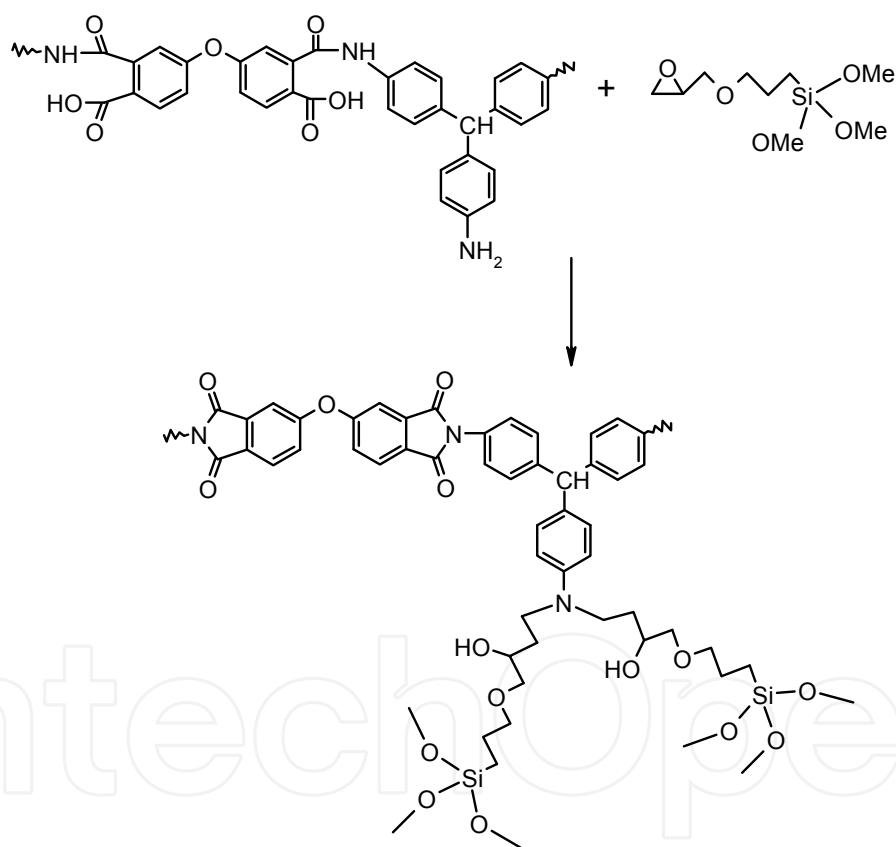


Figure 20. Schematic reaction of the coupling agent 3-glycidyloxypropyltrimethoxysilane with amine end-capped HBPA(O-DPA-MTA)11

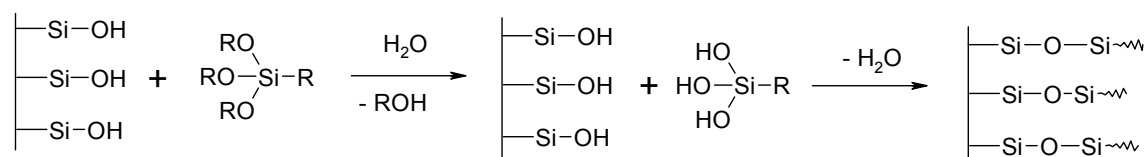


Figure 21. Reaction scheme of the surface hydroxyl groups of silica with alkoxy silanes (OR is an alkoxy group, R is, e.g., glycidyloxypropyl or aminopropyl group)

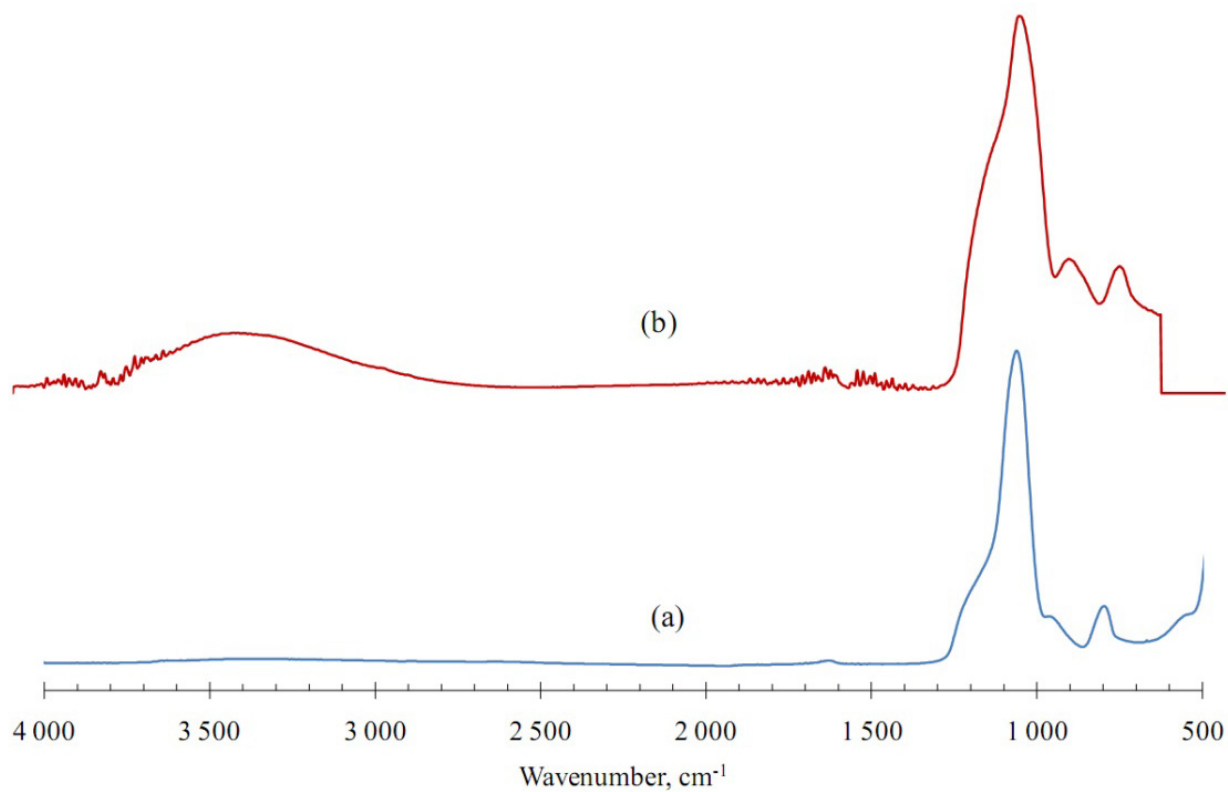


Figure 22. IR spectra of (a) functionalized M-SiO₂-and (b) non-functionalized M-SiO₂ with GPTMS

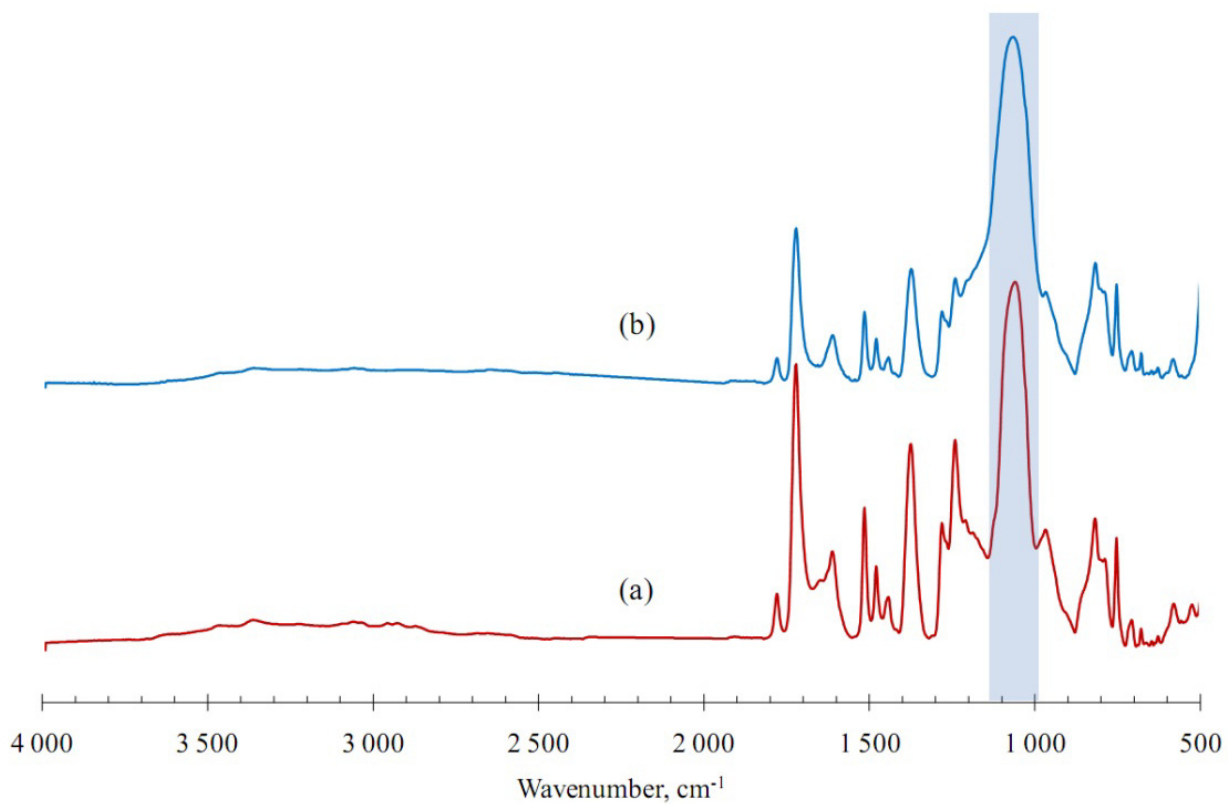


Figure 23. IR spectra of HBPI(ODPA-MTA)11 containing 16 wt% of (a) M-SiO₂, (b) N-SiO₂

The typical photographs of cross-section areas of the mixed matrix materials containing 10 wt% of N-SiO₂ and 16 wt% of M-SiO₂ are shown in Figure 24. It is obvious that the silica particles distribution in the polymer matrix is not regular. Nevertheless, it seems that the porous character of M-SiO₂ (i.e., also its lower specific weight) influenced slightly favourably a silica dispersion. The use of the coupling agent has not brought a more significant improvement. So, these products do not show the morphology of nanomaterials.

The glass transition temperature (Figure 25) and temperatures corresponding to 10 wt% weight loss (Figure 26) change very slightly with both M-SiO₂ and N-SiO₂ content in comparison of these values for pure HBPI(ODPA-MTA)11 (see Figures 16 and 17). It means that the rigidity of polymer chains and the interactions among them are not practically influenced by the silica presence. It is also supported with very similar values of parameter *d* obtained by using wide-angle X-ray diffraction measurements. What concerns transport properties of the flat membranes based on HBPI(ODPA-MTA)11 containing N-SiO₂ our attention was mainly focused on oxygen/nitrogen separation which is connected with a lot problems [9]. It was shown that at the theoretical N-SiO₂ content 10 wt% the permeability coefficients of oxygen and nitrogen decreases semiquantitatively in harmony with a relation

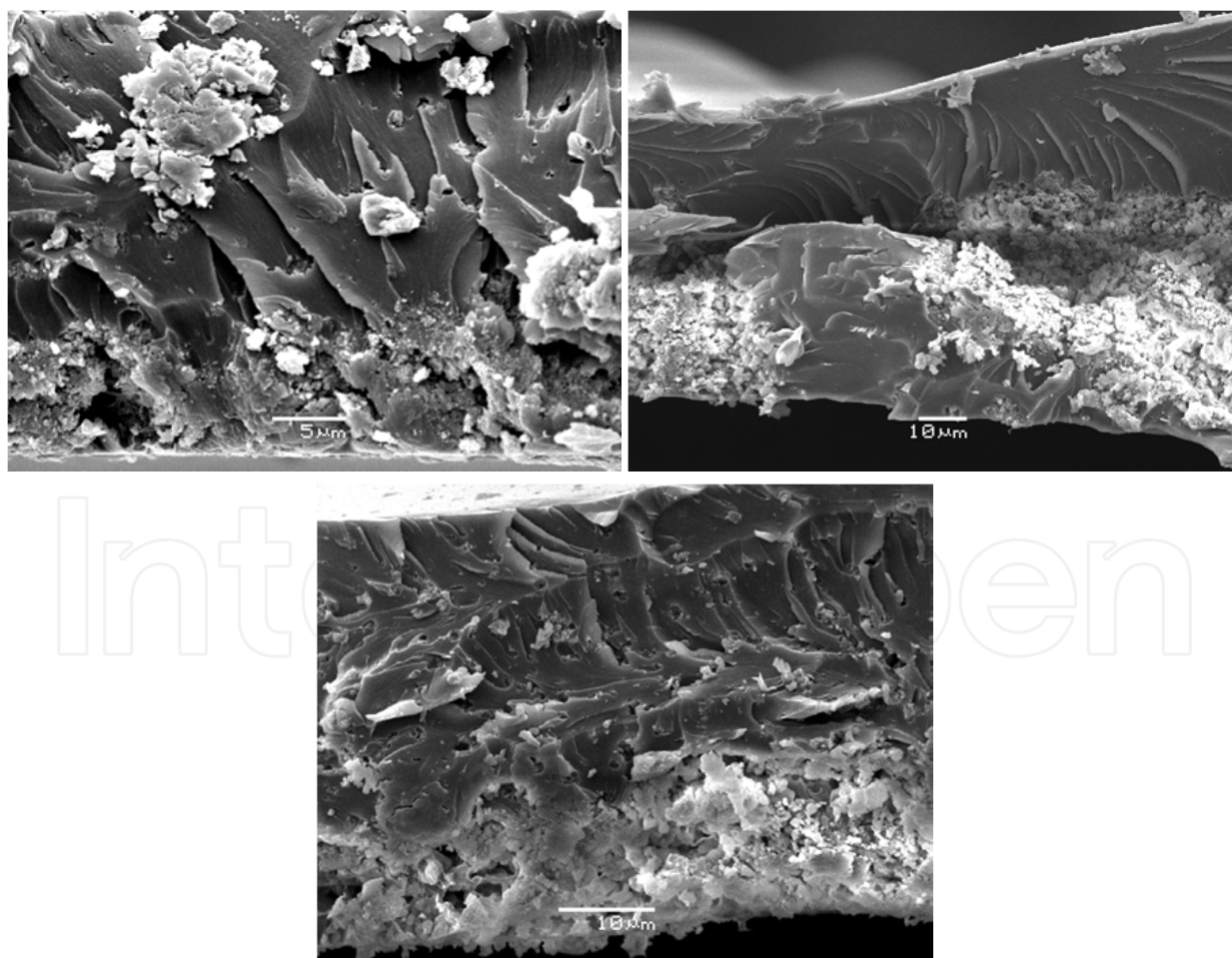


Figure 24. SEM photographs of mixed matrix materials based on HBPI(ODPA-MTA)11 containing (top left) 10 wt% of N-SiO₂, (top right) 10 wt% of M-SiO₂ and (bottom) 16 wt% of M-SiO₂

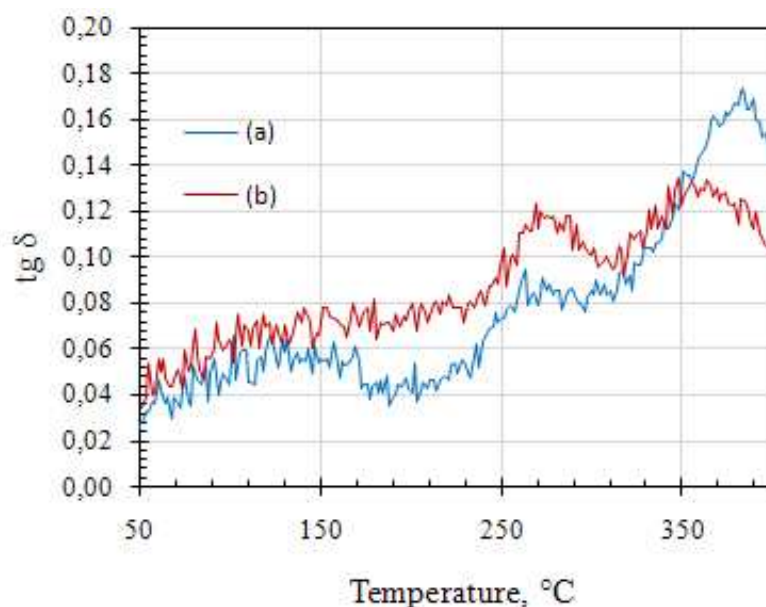


Figure 25. DMA records of mixed matrix materials containing (a) 10 wt% of M-SiO₂; (b) 10 wt% of N-SiO₂

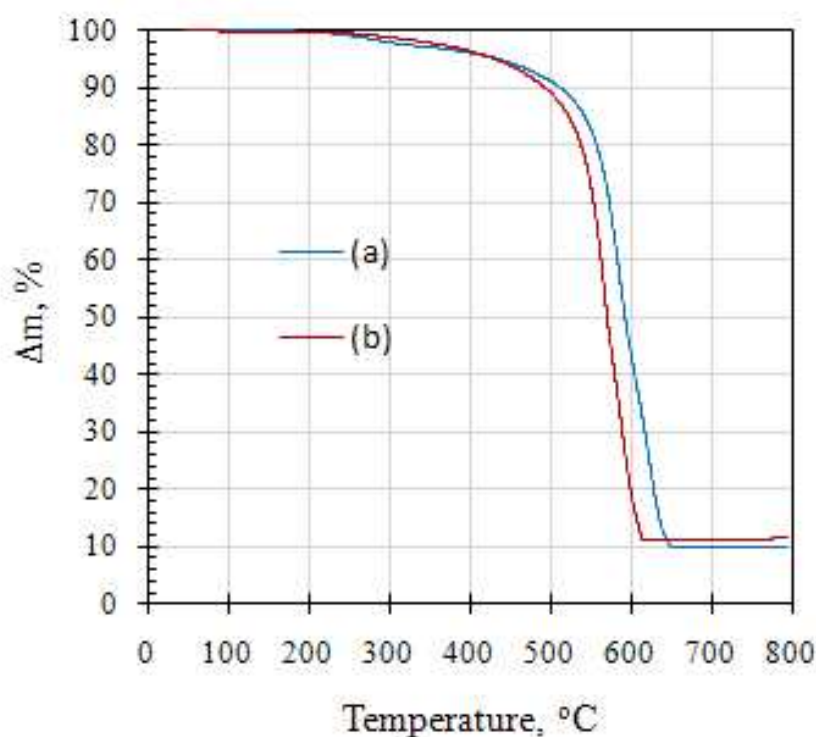


Figure 26. TGA: records of mixed matrix materials based on HBPI(ODPA-MTA)11 containing (a) 10 wt% of M-SiO₂; (b) 10 wt% of N-SiO₂

$P_C = P_{PI} \frac{(1 - \phi_{SiO_2})}{(1 + 0.5\phi_{SiO_2})}$, where P_C is the permeability coefficient of a gas in the matrix mixed membrane, P_{PI} is the permeability coefficient of gas in the pure polyimide matrix and ϕ_{SiO_2} is the silica volume fraction [21]. Due to the fact that the decrease was deeper for

nitrogen, the oxygen/nitrogen selectivity reaches the values higher than 9. Koros [22] explains this difference in oxygen and nitrogen permeabilities by the various levels in their jump frequency reduction. The significant increase of both permeability coefficients (about 80 %) and diffusion coefficients of these gases without change in oxygen/nitrogen selectivity was reached if the organic and inorganic (10 wt%) phases were bound by using 3-glycidyoxypropyltrimethoxysilane. In a such case the upper-bound for the couple oxygen-nitrogen is approached [23]. The importance of the coupling agent (GPTMS) is explained in such case by its contribution to the better distribution of silica particles in the polymer matrix (i.e. a larger interphase area with specific gas separation properties [24]).

The HBPI(ODPA-MTA) are also intended as starting materials for the preparation of membranes for theseparation of racemic mixtures.

4. Conclusion

As the main findings of this work are considered: It has been shown in detail, that

1. the thermooxidative stability of HBPI(ODPA-MTA)₁₁ is lower in comparison with LPI(ODPA-MDA)₁₁
2. the flat membrane prepared from mixed matrix materials based on HBPI(ODPA-MTA)₁₁ and 10 wt% of N-SiO₂ with covalently bound phases approaches the upper bound for the couple oxygen-nitrogen.

Author details

Evgenia Minko, Petr Sysel* and Martin Spergl

Department of Polymers, Institute of Chemical Technology, Prague, Czech Republic

Petra Slapakova

Central Laboratories, Laboratory of Thermal Analysis, Institute of Chemical Technology, Prague, Czech Republic

Acknowledgement

This work was supported by the grant GA CR P106/12/0569 and MSM 6046137302. The financial support from specific university research (MSMT No. 21/2010-013 and 21/2010-011) is also acknowledged.

5. References

- [1] Odian G (2004) Principles of Polymerization. New York: John Wiley & Sons, Inc.

* Corresponding Author

- [2] Tomalia D A (2005) Birth of New Macromolecular Architecture: Dendrimers as Quantized Building Blocks for Nanoscale Synthetic Polymer Chemistry. *Progress in polymer science* 30:294-324.
- [3] Gao C, Yan D (2004) Hyperbranched Polymers: from Synthesis to Applications. *Progress in polymer science*. 29:183-275.
- [4] Jikei M, Kakimoto M (2004) Dendritic Aromatic Polyamides and Polyimides. *Journal of polymer science: part A: polymer chemistry* 42: 1293-1309.
- [5] Hergenrother P M (2003) The Use, Design, Synthesis, and Properties of High Performance/High Temperature Polymers: an Overview. *High performance polymers* 1: 3-45 .
- [6] Hao J, Jikei M, Kakimoto M (2003) Hyperbranched Polyimides Prepared by Ideal $A_2 + B_3$ Polymerization, Non-ideal $A_2 + B_3$ Polymerization and AB_2 Self-polymerization. *Macromolecular symposia* 199: 233-242.
- [7] Fang J, Kita H, Okamoto K (2000) Hyperbranched Polyimides for Gas Separation Applications. 1. Synthesis and Characterization. *Macromolecules* 33:4639-4646.
- [8] Bershtein V A, Egorova L M, Yakushev P N, Sysel P, Hobzova R, Kotek J, Pissis P, Kriptomou S, Maroulas P (2006) Hyperbranched Polyimides Crosslinked with Ethylene Glycol Diglycidyl Ether: Glass Transition Dynamics and Permeability. *Polymer* 47: 6765-6772.
- [9] Bernardo P, Drioli E, Golemme G (2009) Membrane Gas Separation: A Review/State of the Art. *Industrial and engineering chemistry research* 48: 4638-4663.
- [10] Chung T S, Juany L Y, Li Y, Kulprathipanja S (2007) Mixed Matrix Membranes Comprising Organic Polymers with Disperse Inorganic Fillers for Gas Separation. *Progress in polymer science* 32: 483-507
- [11] Fang J, Hidetoshi K, Okamoto K: (2001) Gas Separation Properties of Hyperbranched Polyimide Membranes. *Journal of membrane science* 182: 245-256.
- [12] Sindelar V, Sysel P, Hynek V, Friess K, Sipek M, Castaneda N (2001) Transport of Gases and Organic Vapours through Membranes Made of Poly(amide-imide)s Crosslinked with Poly(ethylene adipate). *Collection of Czech Chemical Communication* 66: 533-540.
- [13] Suzuki T, Yamada Y, Tsujita Y (2004) Gas Transport Properties of 6FDA-TAPOB Hyperbranched Polyimide Membranes. *Polymer* 45: 7167-7171.
- [14] Suzuki T, Yamada Y (2007) Effect of End Group Modification on Gas Transport Properties of 6FDA-TAPOB Hyperbranched Polyimide-Silica Hybrid Membranes *High performance polymers* 19: 553-564.
- [15] Sysel P, Minko E, Cechova R (2009) Preparation and Characterization of Hyperbranched Polyimides Based on 4,4',4''-Triaminotriphenylmethane. *E-Polymers* no. 081.
- [16] Friess K, Sysel P, Minko E, Hauf M, Vopicka O, Hynek V, Pilnacek K and Sipek M (2010) Comparison of Transport Properties of Hyperbranched and Linear Polyimides. *Desalination and water treatment* 14: 165-169.
- [17] Zou H, Wu S, Shen J (2008): Polymer/Silica Nanocomposites: Preparation, Characterization, Properties, and Applications. *Chemical reviews* 108: 3893-3957.

- [18] Reid B D, Ruiz-Trevino F A, Musselman I H, Balkus Jr K J, Ferrari P (2001) Gas Permeability Properties of Polysulfone Membranes Containing the Mesoporous Molecular Sieve MCM-41. *Chemistry of materials* 13: 2366-2373.
- [19] Voit B I, Lederer A (2009) Hyperbranched and Highly Branched Polymer Architecture-Synthetic Strategies and Major Characterization Aspects. *Chemical reviews* 109:5924-5973.
- [20] Sysel P, Minko E, Hauf M, Friess K, Hynek V, Vopicka O, Pilnacek K, Sipek M (2011) Mixed Matrix Membranes Based on Hyperbranched Polyimide and Mesoporous Silica for Gas Separation. *Desalination and water treatment* 34: 211-215.
- [21] Cong H, Radosz M, Towler B F, Shen Y (2007) Polymer-Inorganic Nanocomposite Membranes for Gas Separation. *Separation and purification technology* 55:281-291.
- [22] Moaddeb M, Koros W J (1997) Gas Transport Properties of Thin Polymeric Membranes in the Presence of Silicon Dioxide Particles. *Journal of membrane science* 125: 143-163.
- [23] Robeson L M (2008) The Upper Bound Revisited. *Journal of membrane science* 320: 390-400.
- [24] Chung T S, Jiang L Y, Li Y, Kulprathipanja S (2007) Mixed Matrix Membranes Comprising Organic Polymers with Dispersed Inorganic Fillers for Gas Separation. *Progress in polymer science* 32:483-507.